



OPEN Deep learning reconstruction of diffusion-weighted brain MRI for evaluation of patients with acute neurologic symptoms

Sang Ik Park^{1,2}, Younghee Yim¹✉, Jung Bin Lee¹ & Hye Shin Ahn¹

Purpose: We aimed to evaluate whether the deep-learning (DL) accelerated diffusion weighted image (DWI) is clinically feasible for evaluating patients with acute neurologic symptoms, regarding its shorter study time and acceptable image quality. **Materials and methods:** In this retrospective study, brain images obtained at DWI with a b-value of 0 s/mm² and DWI with a b-value of 1000 s/mm² (DWI 1000) from 321 consecutive patients with acute stroke-like symptom were reconstructed with and without DL algorithm. We compare the diagnostic performance between DL-DWI and conventional DWI for detecting brain lesions, including acute infarction. We assessed the diagnostic accuracy of conventional DWI and DL-DWI and compared the results. Qualitative analysis based on image quality was assessed and compared using a five-point visual scoring system. Apparent diffusion coefficients (ADCs) from DWI with and without DL were also compared. **Results:** The mean acquisition time for the DL-DWI (49 s) was significantly shorter ($P < 0.001$) than conventional DWI (165 s). Both DWI with and without DL showed similar performance in diagnosing brain lesions especially sensitivity (98.8% in both DWI and DL-DWI) and specificity (99.5% in both DWI and DL-DWI). Overall image quality, gray-white matter and deep gray matter differentiation of two sequences were similar. DL DWI showed more artifacts than DWI. Lesion conspicuity, especially smaller than 5 mm, was better with DL DWI than conventional DWI ($p = 0.03$). ADC values of white matter, deep gray matter, and pons with DL were lower than conventional DWI. **Conclusions:** Compared to conventional DWI, DL-DWI achieved comparable image quality and brain lesion visualization for acute neurological symptoms, with a significantly shorter scan time.

Keywords Brain, Acute infarction, Magnetic resonance imaging, Deep learning reconstruction, Diffusion weighted image

Abbreviations

DL	Deep learning
DWI	diffusion weighted image
ADC	apparent diffusion coefficients
MRI	Magnetic Resonance Imaging

Diverse imaging modalities exist for evaluation of stroke. Since its first application in brain Magnetic Resonance Imaging (MRI), diffusion weighted imaging (DWI) became one of the essential and optimal techniques for diagnosing acute ischemic stroke^{1,2}. DWI exhibits tissue characteristics by providing information of the random motion of the water molecules, so-called Brownian movement in biological tissues including tissue cellularity and cell membrane integrity³. A readout signal is generated, dependent on applied diffusion gradients, which is additive to a conventional MR sequence to generate a DWI⁴.

So far, artificial intelligence⁵, machine learning⁶ or deep learning (DL)⁷ have been introduced to help accelerate the reconstruction time and reduce the artifacts. The DL-based reconstruction using a variational network has secured higher acceleration factors for acquisition and improved signal to noise ratio (SNR)^{8,9}. A recent study adopting DL-DWI to liver MRI revealed that DL-DWI was a feasible acquisition technique in clinical routines

¹Department of Radiology, Chung-Ang University Hospital, Chung-Ang University College of Medicine, 102 Heukseok-ro, Dongjak-gu, Seoul, Republic of Korea. ²Department of Radiology, University of Ulsan College of Medicine, Asan Medical Center, Seoul, Korea. ✉email: youngheeyim@gmail.com

and provided improved image quality³. Finally, another study applying DL DWI to prostate cancer revealed that DL DWI could improve the image quality of prostate without affecting the quantification of apparent diffusion coefficients and may potentially improve lesion characterization in patients with suspected prostate cancer¹⁰.

DWI is useful for evaluating episodes of acute atypical or non-focal neurological symptoms, referred to as transient neurological attack (TNA), which pose diagnostic and management challenges in real-world clinical settings¹¹. In this context, enhancing the DWI reliability and speed would be beneficial for efficiently screening patients with ambiguous neurological symptoms, such as dizziness, weakness, paresthesia, loss of consciousness, amnesia, and more. We aimed to evaluate whether the DL DWI is clinically feasible in evaluating the patients with acute neurologic symptoms in terms of image quality and acquisition time when compared with conventional DWI.

Materials and methods

This study compared the image quality and diagnostic performance of conventional DWI and DL-DWI for intracranial lesion and image quality of both sequences. The methods and results have been reported in accordance with the Standards for Reporting of Diagnostic Accuracy Studies (STARD) guidelines¹². All methods were approved by the Chung-Ang University Hospital Institutional Review Board (IRB) No. 2302-014-19457). The requirement for informed consent was waived for this retrospective study and was approved by Chung-Ang University Hospital, IRB.

Study population

This retrospective study included 321 consecutive patients with acute neurologic symptoms from August 2022 to November 2022 who underwent brain DWI images reconstructed with and without DL algorithm (Fig. 1). The inclusion criteria were as follows: (1) patients who underwent DWI with and without DL reconstruction to evaluate transient neurologic attack, and (2) patients without any contraindication to MR. The exclusion criteria were as follows: (1) MR scans with severe motion or metal artifact and (2) imaging data error. Five patients were excluded due to imaging data error ($n=3$), and severe artifact ($n=2$). Thus, 316 patients (156 men and 160 women; mean age, 64.9 years, age range, 20–95 years) were included in this study. The indications for MRI examination were dizziness ($n=107$), weakness ($n=77$), headache ($n=21$), loss of consciousness ($n=20$), and other nonspecific symptoms ($n=91$). We retrospectively surveyed the demographic and clinical data including age, sex, and the final clinical diagnosis using electrical medical record. Three neurologists, each with over 10 years of experience, determined the final diagnosis by comprehensively evaluating all available clinical information, patient progress, and imaging data including follow up DWI. Patients who were symptom-positive but had no corresponding imaging findings were not included in this study.

Image acquisition and reconstruction

All MR examinations were performed on a clinical 3 T scanner (MAGNETOM Vida, Siemens Healthcare, Erlangen, Germany) with patients in the supine position using a 64-channel head and neck array coil. Table 1 provides the detailed MR acquisition parameters of conventional and DL-DWI. The manufacturer provided the prototypical DL-DWI reconstruction for clinical evaluation (Siemens Healthcare, Erlangen, Germany)

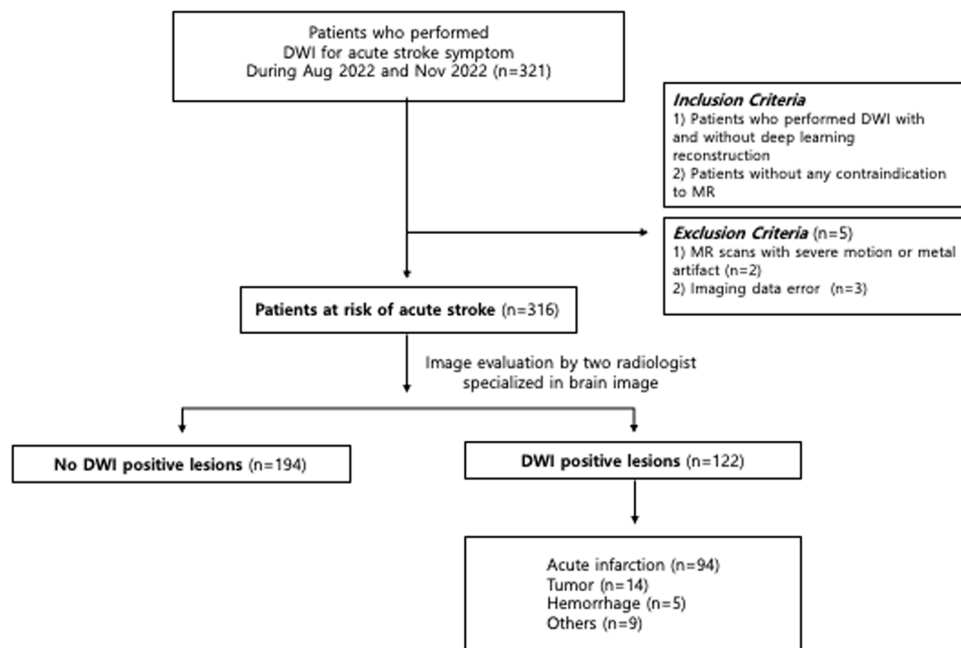


Figure 1. Study flow chart.

	Conventional DWI	DL DWI
b-values (s/mm²)	0/1000	0/1000
TR/TE (ms)	6100/68	6200/69
Field-of-view (mm²)	220×220	230×230
Matrix size	192×192	192×192
In-plane resolution (mm²)	1.15×1.15	1.2×1.2
Slice thickness (mm)	4	4
Number of slices	30	30
Parallel imaging factor	2	3
Number of excitations	1	1
Acquisition time (sec)	165	49

Table 1. Diffusion-weighted imaging parameters. DL DWI indicates diffusion weighted imaging with deep learning reconstruction; TR, repetition time; TE, echo time;

based on previously published methods^{9,13,14,15}. The DL reconstruction of DWI employed a deep learning-based reconstruction scheme, based on a variational network, in which data consistency steps and regularization steps applied. As the first step, k-space to image reconstruction following the idea of a variational network was conducted using precalculated coil sensitivities and acquired single-shot k-space data. The initial 6 iterations applied to focus on data consistency, and 11 iterations additionally employed convolutional neural network-based regularization with hierarchical down-up architecture to focus on denoising. With the corresponding image-to-image neural network, feature maps are extracted. The training was performed in a supervised fashion on approximately 500,000 single-shot DWI images, collected from clinical 1.5 T and 3 T scanners (MAGNETOM, Siemens Healthineers, Erlangen, Germany) and included K-space data of different body regions. The training pairs were generated retrospectively doubling the acceleration factor. For the next step, DL-based reconstructed single-shot images were further processed using an image-based super resolution network to increase spatial resolution. Both reconstruction algorithms were trained offline in a supervised setting using PyTorch. After reconstruction of single-shot images, averaging, trace-weighting, and ADC calculation process were performed analogous to the conventional DWI sequence.

Imaging analysis

Qualitative analysis

Two board-certified radiologists (with seven and five years of experience in neuroradiology) reviewed the two DWI sequences in random order using a picture archiving and communication system and provided subjective scores for overall image quality, gray-white matter differentiation, deep gray matter differentiation using the five-point scale: 1, unacceptable; 2, poor; 3, acceptable; 4, good; 5, excellent. Readers also reported the presence of artifact, diffusion positive lesion, lesion size, lesion conspicuity, and preference between two sequences (1, conventional better; 2, conventional slightly better; 3, equal; 4, DL slightly better; 5, DL better). All radiologists were blinded to the information of conventional or DL sequences, clinical data, and the radiological report.

Lesion assessment

The observers evaluated the presence of DWI-positive lesions, measured the lesion size and subjectively rate the conspicuity of the detected lesions in each DWI using the following 5-point scale: 1, undetectable; 2, poor; 3, acceptable; 4, good; 5, excellent. In case of multiple lesions, the largest one was recorded.

Quantitative analysis

A radiologist with ten years' experience performed quantitative analysis and measured the ADC values of the bilateral centrum semiovale, putamen, temporal white matter, cerebellum and pons and DWI positive lesions on the ADC maps using a manually drawn circular region of interest (ROIs). All ROIs (approximately 0.5 cm²) were placed in the homogeneous brain parenchyma. The ADC values' standard deviations (SD) were also recorded within each ROI. ADC measurements were not performed on the brain parenchyma in one patient because the acute infarction was on the entire right hemisphere of the brain. ADC measurements of focal lesions were only performed when the lesions were larger than 5 mm in diameter due to the limited resolution of the DWIs³. The ROIs in the focal lesions were placed in a homogeneous area, avoiding cystic changes, and covered an area of at least 0.3 mm². ROIs were placed at near-identical locations on images obtained during different sequences, and an average of three ROI measurements was used at each location.

Statistical analysis

All data were analyzed using the software package MedCalc Statistical Software version 19.3.1 (MedCalc Software Ltd, Ostend, Belgium). We assessed the diagnostic accuracy (sensitivity, specificity, accuracy, positive predictive value, and negative predictive value) of conventional DWI and DL-DWI. We utilized the neurologists' final reference diagnosis based on electronic medical records to evaluate diagnostic performance. The qualitative and quantitative imaging parameters were compared using the Wilcoxon signed-rank test. The mean scores of the two observers were used to compare the qualitative scores. Interobserver agreement for qualitative analysis was assessed using weighted κ statistics. A κ value less than 0.20 is considered poor agreement; 0.21–0.40,

		Sensitivity, %	Specificity, %	Accuracy, %	PPV, %	NPV, %
Overall	conventional DWI	98.8	99.5	99.2	99.2	99.2
	DL DWI	98.8	99.5	99.2	99.2	99.2
Obs 1	conventional DWI	98.4	100.0	99.4	100.0	99.0
	DL DWI	98.4	99.5	99.1	99.2	99.0
Obs 2	conventional DWI	99.2	99.0	99.1	98.4	99.5
	DL DWI	99.2	99.5	99.4	99.2	99.4

Table 2. Diagnosis of brain lesions using conventional DWI and DL DWI. DL DWI indicates diffusion weighted imaging with deep learning reconstruction. PPV, positive predictive value. NPV, negative predictive value.

		Conventional DWI	DL DWI	P Value
Overall image quality		4.16 ± 0.47	4.17 ± 0.50	0.77
GW differentiation		4.86 ± 0.42	4.83 ± 0.43	0.21
DG differentiation		4.78 ± 0.44	4.77 ± 0.44	0.70
Artifact	Motion	5.9% (<i>n</i> = 37)	21.5% (<i>n</i> = 136)	< 0.0001
	Others	43.2% (<i>n</i> = 16)	11.0% (<i>n</i> = 15)	
		56.8% (<i>n</i> = 21)	89.0% (<i>n</i> = 121)	
Lesion conspicuity	≤ 5 mm	4.14 ± 0.79	4.58 ± 0.72	0.03
	> 5 mm	4.46 ± 0.76	4.63 ± 0.69	0.02
Lesion conspicuity		4.43 ± 0.77	4.62 ± 0.69	0.005

Table 3. Comparison of qualitative analysis between DL DWI and conventional DWI. Data are mean ± standard deviation and averaged scores of two observers. DL DWI indicates diffusion weighted imaging with deep learning reconstruction. GW: gray-white matter. DG: deep gray matter.

fair agreement; 0.41–0.60, moderate agreement; 0.61–0.80, good agreement; and greater than 0.81, excellent agreement¹⁶.

Results

Study population

Table S1 summarizes the study population and clinical information. We included 316 patients (156 male, 160 female) with mean age of 64.97 ± 16.19 (range 20–95). The neurologic symptoms were dizziness in 33.86% (*n* = 107) patients, weakness in 24.37% (*n* = 77) patients, headache in 6.65% (*n* = 21). 77.05% of patients (*n* = 94) were diagnosed as acute infarction, 11.48% of patients (*n* = 14) were diagnosed as tumor.

Acquisition time

The acquisition time was significantly different between DL DWI and conventional DWI (49 s and 165 s respectively) (*P* < 0.001).

Diagnostic performance and lesion assessment

Two observers detected a total 241 lesions with both conventional and DL DWI among 242 reference lesions. The agreement of lesion detection between the two observers was excellent for both conventional DWI (0.9398) and DL DWI (0.9397). Overall, DL DWI achieved diagnostic performance comparable to that of conventional DWI in terms of sensitivity (conventional DWI vs. DL DWI, 98.8% vs. 98.8%) and specificity (conventional DWI vs. DL-DWI, 99.5% vs. 99.5%). Diagnostic accuracy was also similar in both sequences (Table 2).

Qualitative analysis

Overall, qualitative scores of DWI were similar between conventional DWI and DL-DWI for overall image quality, gray-white matter and deep gray matter differentiation. The lesion conspicuity score for DL-DWI (4.62 ± 0.69) was significantly higher than conventional DWI (4.43 ± 0.77) (*p* = 0.005). When we performed subgroup analysis based on lesion size, lesion conspicuity scores for DL-DWI were higher despite of the size (≤ 5 mm, *p* = 0.03, > 5 mm, *p* = 0.02). More artifacts were reported with DL-DWI (21.5%, *n* = 136) than conventional DWI (5.9%, *n* = 37) (*p* < 0.0001, Table 3). When we analyzed the specific cause of the artifacts, motion artifacts were reported in a similar number of cases for both conventional and DL DWI (*n* = 16 and *n* = 15, respectively). However, DL-DWI exhibited significantly more susceptibility artifacts, such as blurring near the vertex. The agreement between the two observers was fair to good, with a weighted κ ranging from 0.5156 to 0.7871 for DL DWI and 0.5787–0.6520 for conventional DWI. When comparing the two sequences, readers indicated an equal preference in 76.3% (482 out of 632 observations) of cases, and conventional DWI and DL DWI were preferred in 11.8% (75 out of 632 observations) of cases, respectively.

		Conventional DWI	DL DWI	P Value
Centrum semiovale	Right	0.76 ± 0.08	0.71 ± 0.08	< 0.0001
	Left	0.77 ± 0.08	0.73 ± 0.09	< 0.0001
Putamen	Right	0.74 ± 0.10	0.65 ± 0.12	< 0.0001
	Left	0.74 ± 0.11	0.65 ± 0.12	< 0.0001
Temporal lobe	Right	0.80 ± 0.08	0.80 ± 0.07	0.8422
	Left	0.84 ± 0.08	0.80 ± 0.07	< 0.0001
Pons		0.78 ± 0.09	0.73 ± 0.09	< 0.0001
Cerebellum	Right	0.68 ± 0.05	0.67 ± 0.06	0.6756
	Left	0.68 ± 0.05	0.68 ± 0.06	0.0729

Table 4. Comparison of ADC Measurement ($\times 10^{-3}$ mm²/s) in Brain Parenchyma. Data are mean \pm standard deviation. DL DWI indicates diffusion weighted imaging with deep learning reconstruction.

	Conventional DWI	DL DWI	P Value
	0.66 ± 0.36	0.59 ± 0.36	< 0.0001
Acute infarction	0.56 ± 0.13	0.49 ± 0.14	< 0.0001
Tumor	1.16 ± 0.60	1.08 ± 0.57	0.0041
Hemorrhage	0.96 ± 0.74	0.87 ± 0.79	0.0836
<i>Subgroup analysis</i>			
Infarction vs. tumor	$P < 0.0001$	$P < 0.0001$	
Infarction vs. hemorrhage	$P < 0.0001$	$P = 0.0002$	
Tumor vs. hemorrhage	$P = 0.5611$	$P = 0.5434$	

Table 5. Lesion ADC measurement ($\times 10^{-3}$ mm²/s). Data are mean \pm standard deviation. DL DWI indicates diffusion weighted imaging with deep learning reconstruction.

Quantitative analysis

The ADC values in the temporal white matter were the highest while those of cerebellum showed the lowest values. The ADC values calculated with DL-DWI were consistently lower in both centrum semiovale, putamen, left temporal white matter, pons and cerebellum ($P < 0.001$) (Table 4). Within each ROI, the SD were significantly lower in DL-DWI than in conventional DWI (all, $P < 0.001$) (Table S2).

One hundred five lesions received ADC measurement (acute infarction = 82, tumor = 13, hemorrhage = 5, others = 5) and overall ADC value measured with DL-DWI was significantly lower than that of conventional DWI ($P < 0.001$). In subgroups analysis, ADC values measured with DL-DWI were significantly lower in acute infarction and tumor ($P < 0.001$, $P = 0.0041$). In both sequences, acute infarction lesions demonstrated significantly lower ADC values than tumor or hemorrhage (DL-DWI, $P < 0.001$, $P = 0.0002$; conventional DWI, $P < 0.001$) (Table 5).

Discussion

In this study, we demonstrated similar diagnostic accuracy of DL-DWI and conventional DWI for the evaluation of patients with acute neurologic symptoms. With DL, we acquired feasible and reliable DWI images covering the whole brain in less than one minute, which is less than one third of the scan time of conventional DWI. DL-DWI demonstrated similar diagnostic performance without hampering the overall image quality. Lesion conspicuity is better with DL-DWI even though more artifacts were reported with DL-DWI.

One of the greatest advantage adopting DL reconstruction to DWI is time reduction, which naturally improves patient comfort and overall experience¹⁷. Although MR is one of the most essential imaging modalities to diagnosing various neurologic disease, not every patient is amenable to the study due to its uncomfortable noise and long scan time. Remaining within an enclosed space and enduring loud noise can make patients and clinicians reluctant to evaluate symptoms, especially when no acute stroke is strongly suspected. One study reported that up to 30% of patients experienced significant anxiety due to claustrophobia during MR study¹⁸.

Additionally, MR is susceptible to image degradation from patient movement related to long scan time. According to the previous report, about 29% of inpatient/emergency department examination and 7% of outpatient studies face challenges arising from the movement, which leads to the repeated examination with significantly increased financial burden^{19,20}. In our study achieved a scan time reduction of approximately 70% while maintaining overall quality. Although our study results indicated more artifacts with DL-based DWI, most were due to susceptibility rather than motion. We expect these issues to be overcome with advancements in the algorithm. If DL-reconstructed fast protocols were utilized with other sequences, one could anticipate an improvement in exam-related workflow efficiency for an imaging facility. Also, with shorter scan time, high sensitivity DWI can detect and evaluate possible cerebrovascular risk earlier (Fig. 2).

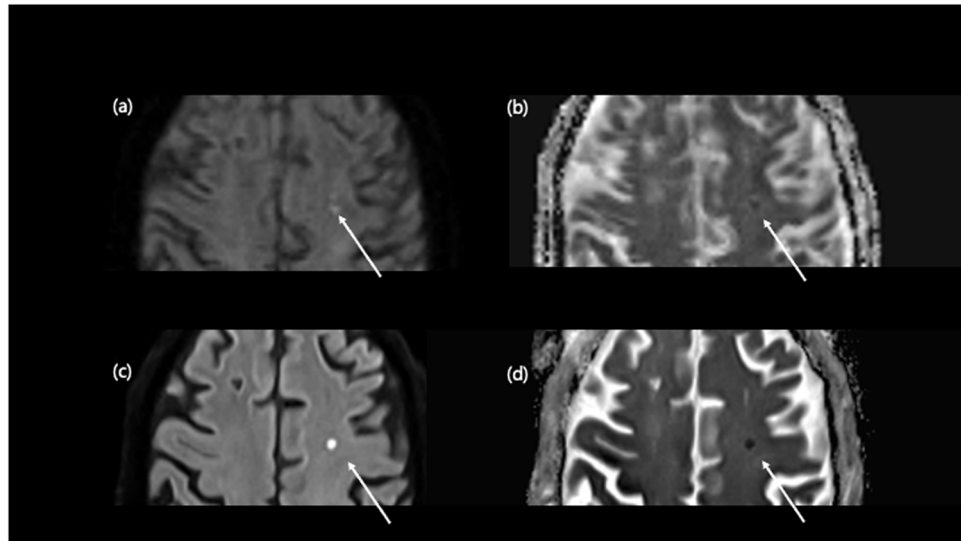


Figure 2. Comparison of small acute infarction on conventional DWI and DL-DWI. A 71-year-old male visited the emergency room complaining transient right-sided weakness. Conventional DWI revealed a small (≤ 5 mm) indistinct DWI high-signal-intensity lesion in the left frontal lobe (a) with a severely blurred ADC map (b) due to motion artifact. However, DL-DWI demonstrated a discrete lesion (c) with clear ADC map (d).

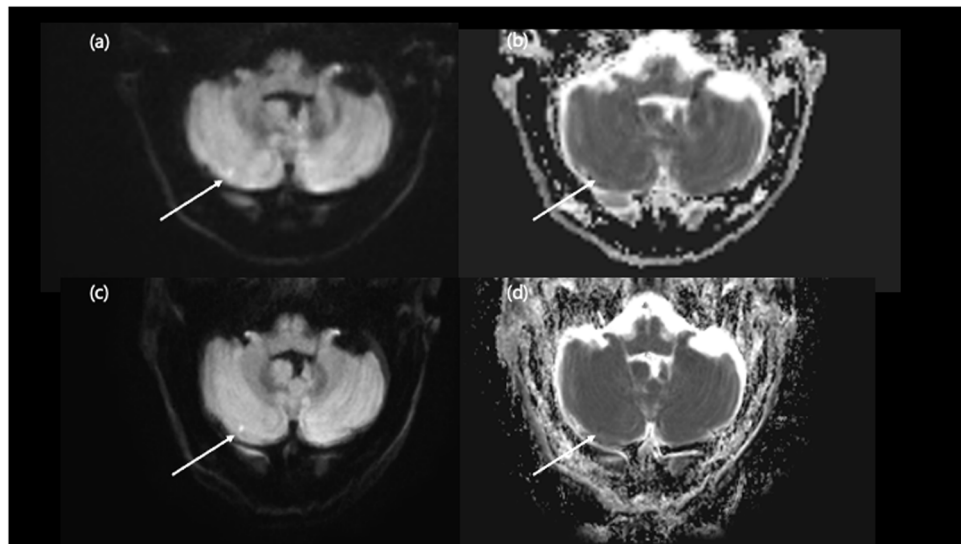


Figure 3. Comparison of embolic infarction on conventional DWI and DL-DWI. A 78-year-old male visited the emergency room after resuscitation of cardiac arrest. Conventional DWI revealed a small (≤ 5 mm) indistinct DWI high-signal-intensity lesion in right cerebellum (a) with blurred ADC map which does not clearly describe the lesion correlated with the DWI (b). However, with DL-DWI, the lesion had more discrete margin (c) with clear ADC map, so we could diagnose tiny embolic infarction (d).

Along with the shortened scan time, DL DWI achieved better lesion conspicuity than conventional DWI (Figs. 3, 4, 5 and 6). This finding aligns with a previous study, which revealed that DL-DWI produced better overall image quality and sharper organ anatomic details in the liver and pancreas with less noise and artifact³. DL has emerged as a promising tool for strengthen the MRI image quality. Previous studies adopted DL techniques to reduce noise, enhance contrast, and boost the special resolution²¹. DL-DWI proves invaluable for enhancing diagnostic confidence, particularly in uncertain acute clinical situations. It excels in delivering highly sensitive imaging for intracranial lesions of small size (≤ 5 mm), ensuring improved lesion conspicuity with distinct margins due to reduced noise and artifacts compared to conventional DWI. DWI is useful to evaluate the microscopic water diffusion rate within the tissue, which alters with variety of disease processes²² and is one of the most important sequence in lesion detection²³ or screening for stroke. In that sense, the excellent ability to

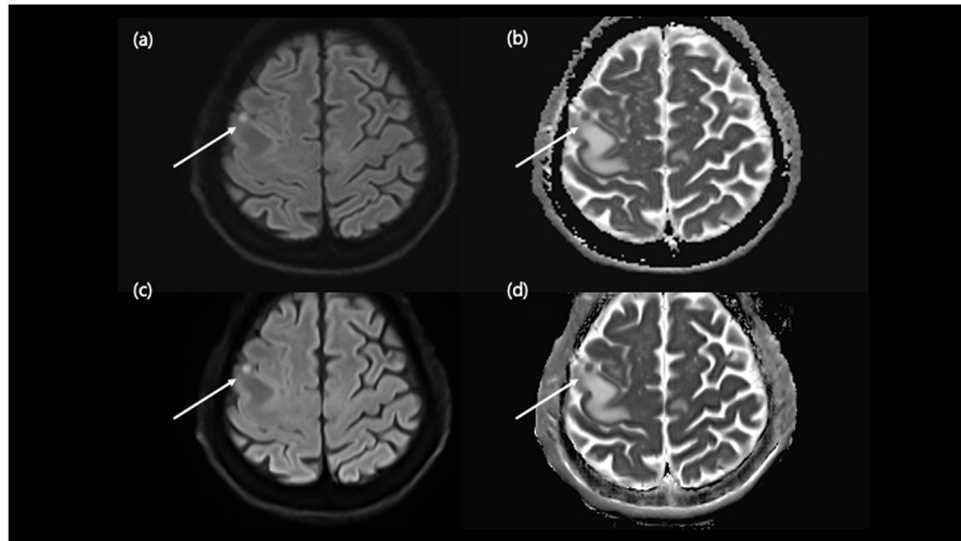


Figure 4. Comparison of tumor on conventional DWI and DL-DWI. A 63-year-old male visited the emergency room with symptom of transient left facial palsy. Conventional DWI shows a small DWI high-signal-intensity lesion in the right frontal cortex (a) with low ADC value (b) with perilesional edema. DL-DWI (c) demonstrated that this discrete nodular lesion had low value on ADC map (d), and the patient was diagnosed with a metastatic tumor.

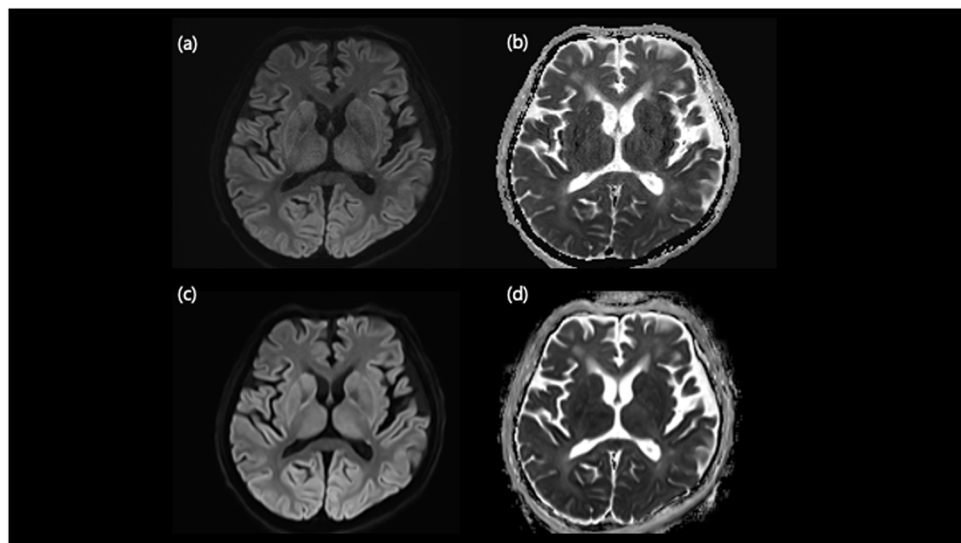


Figure 5. Comparison of hypoxic ischemic encephalopathy on conventional DWI and DL-DWI. An 86-year-old male visited the emergency room with an altered mentality. Conventional DWI revealed subtle DWI high-signal-intensities in bilateral basal ganglia, thalami, and cerebral cortex (a) with an equivocal ADC value change (b). Correlated location clearly demonstrated on DL-DWI (c) with ADC value changes (d), and the patient was diagnosed with hypoxic-ischemic-encephalopathy.

differentiate these small lesions with highly sensitive DL-DWI could enable it to be used as an initial screening tool for patients with ambiguous neurologic symptoms.

In this study, ADC values of DL DWI were consistently lower than those of conventional DWI. Furthermore, the SDs of DL-DWI ADC measurement were significantly lower for all brain locations than those of conventional DWI. The lower SD indicates that the ADC values are less scattered and more reliable in the ROI. Several studies reported that superior DWI protocols produced lower SDs for ADC measurement³, and a study demonstrated SD of ADC ROIs had a negative correlation with visibility in DWI²⁴. Also, the ADC values of focal lesions were consistently lower with DL-DWI than conventional DWI, which aligns with previous study³. This result is not fully understood, but we believe that possible differences in acquisition protocol between two DWIs might affect

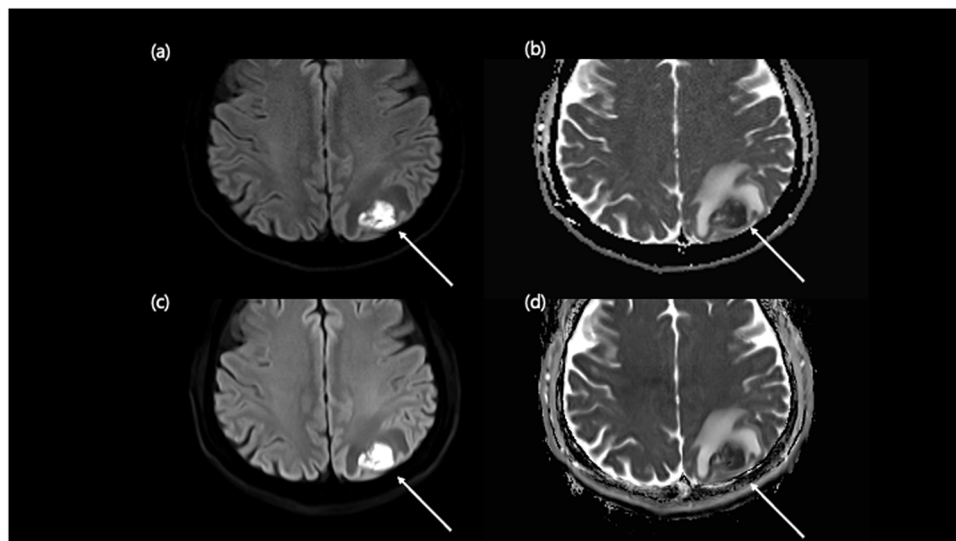


Figure 6. Comparison of brain abscess on conventional DWI and DL-DWI. A 64-year-old male visited emergency room with seizure. Conventional DWI revealed an approximately 2cm lobulated contour, diffusion restricted lesion with perilesional edema in the left parietal lobe (a, b). With DL-DWI, the lesion clearly demonstrated better contrast (c, d), leading to brain abscess diagnosis.

the ADC values. However, no solid ground exists for assessing ADC values with DL reconstruction. Future studies are needed to assess ADC measurements in DL reconstruction images.

Our study has several limitations. First, selection bias could exist because this study was performed at a single referral center with relatively few patients. Further study with larger sample size will be beneficial for the validation of DL-DWI. Second, although the neuroradiologists providing ratings were blinded to the pulse sequence during the evaluation, they might have noticed the imaging features of each sequence, which could cause observer bias. Moreover, the acquisition order could have affected image quality, considering that images acquired later in the examination could have more motion artifacts. We tried to minimize bias by (1) randomizing the order of acquisition during the study and (2) undergoing not only qualitative analyses but also quantitative evaluation. Third, the readers were all experienced neuroradiologists, which could affect the diagnostic performance. It would be beneficial to involve readers who are in various stage of experience in neuroimaging to investigate more realistic clinical feasibility. Forth, intracranial lesions were not confirmed pathologically, but diagnosed patients by clinically with imaging. This might impact diagnostic performance; however, we mitigated errors by making the final diagnosis through a comprehensive evaluation of all available clinical information, patient progress, and imaging data. Also, we did not account for patients with negative imaging but positive symptoms, which could introduce bias in false-negative cases such as transient ischemic attack. However, this study is focused solely on comparing the two sequences in cases where a positive lesion is present on DWI. Finally, the ADC value can be influenced by specific ROIs, despite our efforts to minimize errors, especially within the positive lesion such as acute infarction or tumors. However, we compared the ADC values to analyze trends between conventional DWI and DL-DWI, rather than comparing absolute values. Larger data studies are needed for standardization.

DWI is one of the most important imaging for diagnosing a wide range of neurologic symptoms to promote early intervention¹¹. However, its relatively long examination time and relatively limited accessibility remain significant disadvantages. In this study, we speculated that DL-DWI achieved comparable image quality and visualization of brain lesions for acute neurological symptoms, with a significantly shorter scan time than conventional DWI. Examination time reduction could be one essential step towards providing DWI for an increasing number of patients, yielding enormous potential for screening and early intervention for possible cerebrovascular events.

Data availability

The datasets used and/or analysed during the current study available from the corresponding author on reasonable request, but there could be certain process to release the data due to the local policy.

Received: 20 May 2024; Accepted: 1 October 2024

Published online: 21 October 2024

References

1. Le Bihan, D. et al. MR imaging of intravoxel incoherent motions: application to diffusion and perfusion in neurologic disorders. *Radiology*. **161**, 401–407 (1986).
2. Sevick, R. et al. in *Brain Edema VIII: Proceedings of the Eighth International Symposium, Bern, June 17–20, 1990*. 210–212 (Springer).

3. Bae, S. H. et al. Clinical feasibility of accelerated diffusion weighted imaging of the abdomen with deep learning reconstruction: comparison with conventional diffusion weighted imaging. *Eur. J. Radiol.* **154**, 110428 (2022).
4. Mori, S. & Barker, P. B. Diffusion magnetic resonance imaging: its principle and applications. *Anat. Record: Official Publication Am. Association Anatomists.* **257**, 102–109 (1999).
5. Schilling, K. G. & Landman, B. A. AI in MRI: a case for grassroots deep learning. *Magn. Reson. Imaging.* **64**, 1 (2019).
6. Castellazzi, G. et al. A machine learning approach for the differential diagnosis of Alzheimer and vascular dementia fed by MRI selected features. *Front. Neuroinform.* **14**, 25 (2020).
7. Zhu, G. et al. Applications of deep learning to neuro-imaging techniques. *Front. Neurol.* **10**, 869 (2019).
8. Schlemper, J., Caballero, J., Hajnal, J. V., Price, A. N. & Rueckert, D. A deep cascade of convolutional neural networks for dynamic MR image reconstruction. *IEEE Trans. Med. Imaging.* **37**, 491–503 (2017).
9. Hammernik, K. et al. Learning a variational network for reconstruction of accelerated MRI data. *Magn. Reson. Med.* **79**, 3055–3071 (2018).
10. Ueda, T. et al. Deep learning reconstruction of diffusion-weighted MRI improves image quality for prostatic imaging. *Radiology.* **303**, 373–381 (2022).
11. van Rooij, F. G. et al. Diffusion-weighted imaging in transient neurological attacks. *Ann. Neurol.* **78**, 1005–1010 (2015).
12. Cohen, J. et al. STARD 2015 guidelines for reporting diagnostic accuracy studies: explanation and elaboration. *BMJ Open* **6**, e012799. <https://doi.org/10.1136/bmjopen-2016-012799> (2016).
13. Chen, F. et al. Variable-density single-shot fast spin-echo MRI with deep learning reconstruction by using variational networks. *Radiology.* **289**, 366–373 (2018).
14. Altmann, S. et al. Deep learning accelerated brain diffusion-weighted MRI with super resolution processing. *Acad. Radiol.* S1076–6332 (2024).
15. Jeong, J. et al. Deep learning image reconstruction of diffusion-weighted imaging in evaluation of prostate cancer focusing on its clinical implications. *Quant. Imaging Med. Surg.* **14**, 3432 (2024).
16. Landis, J. R. & Koch, G. G. An application of hierarchical kappa-type statistics in the assessment of majority agreement among multiple observers. *Biometrics* **33**(2), 363–374 (1977).
17. Bash, S. et al. Deep learning image processing enables 40% faster spinal MR scans which match or exceed quality of standard of care: a prospective multicenter multireader study. *Clin. Neuroradiol.* **32**, 197–203 (2022).
18. Meléndez, J. C. & McCrank, E. Anxiety-related reactions associated with magnetic resonance imaging examinations. *Jama.* **270**, 745–747 (1993).
19. Zaitsev, M., Maclaren, J. & Herbst, M. Motion artifacts in MRI: a complex problem with many partial solutions. *J. Magn. Reson. Imaging.* **42**, 887–901 (2015).
20. Andre, J. B. et al. Toward quantifying the prevalence, severity, and cost associated with patient motion during clinical MR examinations. *J. Am. Coll. Radiol.* **12**, 689–695 (2015).
21. Matsuo, K. et al. Feasibility study of super-resolution deep learning-based reconstruction using k-space data in brain diffusion-weighted images. *Neuroradiology.* **65**, 1619–1629 (2023).
22. Choi, D. S. Bright intracranial lesions on diffusion-weighted images: a pictorial review. *J. Korean Radiological Soc.* **55**, 21–32 (2006).
23. Castillo, M. & Mukherji, S. K. in *Seminars in Ultrasound, CT and MRI.* 405–416 (Elsevier).
24. Metens, T. et al. Normal hepatic parenchyma visibility and ADC quantification on diffusion-weighted MRI at 3 T: influence of age, gender, and iron content. *Eur. Radiol.* **24**, 3123–3133 (2014).

Acknowledgements

InSeong Kim at Siemens Healthcare Ltd., Seoul, South Korea, helped to install, optimize scan parameters and answer technical questions of DL-DWI. This work was supported by the National Research Foundation of Korea (NRF) grant funded by the Korea government (MSIT) (No. RS-2023-00274981).

Author contributions

All authors contributed to the study conception and design. Material preparation, data collection and analysis were performed by HS Ahn and JB Lee. The first draft of the manuscript was written by SI Park and Y Yim and all authors commented on previous versions of the manuscript. All authors read and approved the final manuscript.

Declarations

Competing interests

The authors declare no competing interests.

Additional information

Supplementary Information The online version contains supplementary material available at <https://doi.org/10.1038/s41598-024-75011-1>.

Correspondence and requests for materials should be addressed to Y.Y.

Reprints and permissions information is available at www.nature.com/reprints.

Publisher's note Springer Nature remains neutral with regard to jurisdictional claims in published maps and institutional affiliations.

Open Access This article is licensed under a Creative Commons Attribution-NonCommercial-NoDerivatives 4.0 International License, which permits any non-commercial use, sharing, distribution and reproduction in any medium or format, as long as you give appropriate credit to the original author(s) and the source, provide a link to the Creative Commons licence, and indicate if you modified the licensed material. You do not have permission under this licence to share adapted material derived from this article or parts of it. The images or other third party material in this article are included in the article's Creative Commons licence, unless indicated otherwise in a credit line to the material. If material is not included in the article's Creative Commons licence and your intended use is not permitted by statutory regulation or exceeds the permitted use, you will need to obtain permission directly from the copyright holder. To view a copy of this licence, visit <http://creativecommons.org/licenses/by-nc-nd/4.0/>.

© The Author(s) 2024